Chinese Journal of Electronics
Vol.32, No.4, July 2023

Multi-Frequency-Ranging Positioning Algorithm for 5G OFDM Communication Systems

LI Wengang[1], XU Yaqin[1], ZHANG Chenmeng[1], TIAN Yiheng[1], LIU Mohan[1], and HUANG Jun[2]

(1. *State Key Laboratory of Integrated Services Networks, College of Communication Engineering, Xidian University, Xi'an 710000, China*)

(2. *Electronic Countermeasures Academy, National University of Defense Technology, Hefei 230601, China*)

Abstract — The accurate determination of vehicle location is of great research significance, considering challenges such as the multipath environment and the absence of Global Navigation Satellite System (GNSS) signals. In this particular environment, vehicles equipped with 5G wireless communication devices can enhance their positioning accuracy by exchanging information with infrastructure (vehicle-to-infrastructure, V2I). Therefore, in this paper, we propose a multifrequency ranging method and positioning algorithm specifically designed for 5G orthogonal frequency division multiplexing (OFDM) communication systems. Our approach involves selecting specific subcarriers within the OFDM communication system for transmitting ranging frames and capturing delay observations. Importantly, this selection does not affect the functionality of other subcarriers used for regular communication. By utilizing dedicated subcarriers for ranging and positioning, we achieve accurate vehicle location without significantly impacting communication capacity. We outline the method for selecting ranging subcarriers and describe the format of the ranging frame carried by these subcarriers. To evaluate the effectiveness of our system, we prove the Cramér-Rao lower bound of this ranging positioning system. The obtained ranging positioning accuracy meets the requirements for vehicle location applications. In our experimental simulations, we compare the performance of our system with other positioning methods, demonstrating its superiority. Additionally, we provide theoretical proofs and simulations that establish the relationship between ranging accuracy and channel parameters in a multipath environment. The simulation results indicate that, under the conditions of a 5 GHz frequency and a high signal-to-noise ratio, our system achieves a positioning accuracy of approximately 5 cm.

Key words — Vehicle location, 5G, Orthogonal frequency division multiplexing, Multi-frequency ranging.

I. Introduction

With the development of society, location-based service (LBS) has become more and more important. For example, robot positioning, vehicle automatic driving, and indoor rescue [1], all require precise position information. In fact, accurate position information is the basis for developing LBS. At present, the increasingly mature Global Navigation Satellite System (GNSS) achieves sub-meter outdoor positioning accuracy [2], and the development of real-time kinematic (RTK) technology improves the positioning accuracy to the centimeter level with the help of ground-assisted stations [3].

Currently, significant efforts are being made to enhance the accuracy, robustness, and reliability of positioning systems while ensuring high real-time performance. Many researchers are dedicated to the exploration and development of positioning systems that integrate both internal and external vehicle information [4]–[6]. By equipping vehicles with wireless communication devices, they can effectively exchange data with the surrounding environment, enabling seamless communication between vehicles and the Internet, vehicle-to-vehicle (V2V) communication, vehicle-to-sensor communication, as well as vehicle-to-infrastructure (V2I) communication. These interactions allow vehicles to acquire external information from nearby vehicles or fixed infrastructure units located on the roadside [7]. Information fusion between existing positioning methods and vehicle positioning related information obtained through a communication system can further improve the performance of the positioning system. Moreover, it offers a solution to mitigate the limitations of on-vehicle

Manuscript Received Apr. 9, 2021; Accepted Mar. 11, 2022. This work was supported by the National Natural Science Foundation of China (U21A20446).

 DOI:10.23919/cje.2021.00.124

sensors caused by restricted viewing distances. This approach broadens the possibilities for optimizing and improving positioning systems in the future, while requiring relatively affordable costs.

However, it is important to note that GNSS-based positioning is ineffective indoors as satellite signals cannot penetrate buildings. This creates an urgent demand for alternative location-based services in various activities. When GNSS is unable to provide positioning services, there is a growing research focus on obtaining accurate location information in complex geographical environments. Both industry and academia are actively seeking high-precision and high-reliability positioning, technologies to address this challenge and ensure accurate location information in such environments.

In certain specific scenarios where the available space is limited, the cellular network-based partition positioning method [8] may not offer sufficient accuracy for positioning. Although the radio frequency identification (RFID) positioning method [9] provides high accuracy, it is constrained by short positioning distances and requires specialized equipment. Ultra-wideband (UWB) is a commonly utilized positioning technology [10] that offers various positioning algorithms based on UWB ranging [11]. For instance, pseudo-random codes are employed for positioning in orthogonal frequency division multiplexing (OFDM) systems [12]. Notably, channel state information (CSI) can be leveraged for distance measurement, leading to the proposal of CSI-based Cramer-Rao lower bound (CRLB) in UWB positioning research. Theoretical investigations on positioning performance in multipath environments are also conducted. Additionally, the utilization of fingerprint characteristics in positioning technology is a prominent area of research. Machine learning techniques are employed to exploit channel state information [13], received signal strength indicator [14], and other relevant characteristics for accurate localization. However, this method requires data collection and network training in advance, which has greater limitations.

Wireless positioning technologies are mainly divided into two categories: ranging-based technologies that measure propagation delay and non-ranging technologies that use matching fingerprints, among which ranging-based technologies are the first choice for lower cost. Because of its good anti-multipath performance, OFDM technology can be used to improve the accuracy of ranging and positioning. In [15] and [16], the CRLB based on OFDM was investigated. Reference [15] focused on the single-path channel and found that the performance of OFDM was limited in that context. In contrast, reference [16] explored ranging in the frequency domain and obtained range estimates for multipath channels. Literature [17] proved that with the same positioning accuracy, non-data-bearing OFDM (NDB OFDM) in wireless positioning is more energy-efficient than non-pulse-shaping pseudo-random noise (NPS PN) currently widely used in satellites and the ground. Articles [18], [19] improve positioning accuracy by optimizing network and carrier power allocation. But the signal power to locate the channel has higher requirements. Many positioning algorithms are based on ranging information, such as the least squares algorithm [20] and the chan algorithm [21]. Wang [22] proves the bound of position estimation in 3-D localization is closely associated with the bound of range estimation. That means the accuracy of distance measurement guarantees the accuracy of positioning.

Among the three scenarios of 5G, except eMBB (enhanced mobile broadband) for human network, the other two scenarios are Internet of things (IoT) scenarios: mMTC (massive machine communication) is for low power consumption and large capacity, and is widely used in smart cities; URLLC (ultra-reliable, low-latency communication) pursues high reliability and low latency, and is mainly used in the industrial field. Taking into account factors such as cost, power efficiency, and usage scenarios, the majority of mMTC IoT terminals are designed to be compact and do not include GNSS chips. Consequently, these terminals rely on positioning technologies provided by network operators. Therefore, the positioning demands of numerous mMTC IoT terminals will significantly expand the application scenarios for operators' 5G location services. The proposed method can effectively leverage the capabilities of a 5G communication system, offering improved performance and enhancing the overall functionality of the system.

In wireless positioning, the presence of multipath signals often results in poor positioning accuracy. To address this issue, this paper proposes a multi-carrier ranging and positioning system based on OFDM. By leveraging the advantages of OFDM, this system aims to mitigate the impact of multipath effects and enhance positioning accuracy. Specifically, the proposed OFDM system integrates communication and positioning functionalities, utilizing a triple-frequency positioning method to improve accuracy and stability. This approach achieves high positioning accuracy while minimizing the impact on communication capacity, thus catering to the requirements of positioning applications.

The contributions of this paper can be summarized as follows.

1) Select three subcarriers in an OFDM communication system, and introduce the selection method and the format of the ranging frame carried by the subcar-

riers.

2) We focus on OFDM systems and derive the bounds for OFDM ranging accuracy in multipath channels based on Fisher information analysis. Prove the EFI of multi-frequency ranging and how it is affected by the channel parameters.

3) The simulation experiments conducted in this paper validate the results obtained through theoretical derivation. Furthermore, the ranging positioning performance is compared with that of other positioning methods. The study examines how the accuracy of ranging and positioning is affected by variations in channel parameters, thus providing empirical evidence and insights into the impact of these changes on the accuracy of the system.

II. OFDM System

OFDM technology is widely used in 4G, 5G and other high-speed communication systems. The wireless local area network IEEE 802.11a standard, the wireless metropolitan area network IEEE 802.16 standard, etc., all adopt OFDM as the core technology. OFDM is a frequency division multiplexing technique based on multi-carrier modulation. Multiple subcarriers overlap each other orthogonally in frequency to form multiple subchannels, as shown in Fig.1. Through serial-to-parallel conversion, the input high-rate data information stream is converted into multiple low-rate data information streams that are transmitted in parallel, while the broadband is converted into multiple identical narrowbands, and the parallel data streams are transmitted on narrowband subchannels. Under normal communication conditions, the signal bandwidth of an OFDM system is less than the relevant bandwidth of the channel. Therefore, the fading of each subchannel is consistent with flat fading, so it has good resistance to multipath.

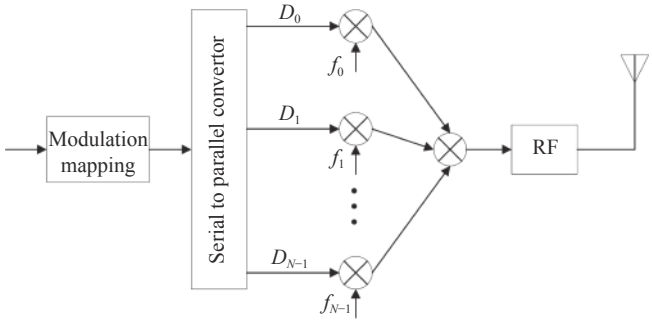

Fig. 1. OFDM modulation process.

1. OFDM modulation and demodulation

OFDM modulation method is shown in Fig.1, "Serial to parallel conventor" converts a high-speed data stream into N sets of parallel data blocks D_0–D_{N-1}, and modulate each data block with subcarriers f_0–f_{N-1} respectively. The modulated subcarrier signals of the N parallel branches are added to obtain the actual transmitted signal of the OFDM.

As shown in Fig.2, at the receiving end, the received signal enters N parallel branches at the same time, and can be restored by multiplying and integrating (coherent demodulation) with N subcarriers, respectively. Parallel data is merged into serial data through "Parallel-to-serial conventor".

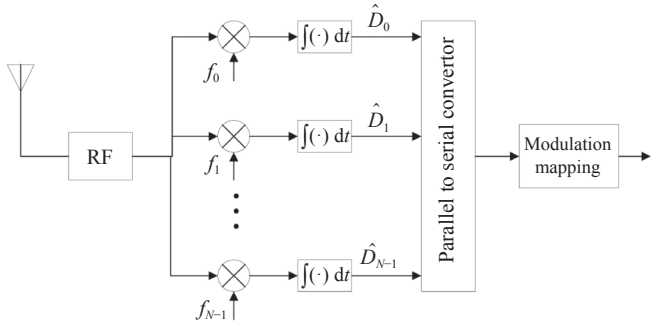

Fig. 2. Receiver OFDM demodulation process.

2. Channel fading

If the channel has a constant gain and the linear phase response bandwidth is smaller than the bandwidth of the transmitted signal, then this channel characteristic will cause frequency selective fading of the received signal. In this case, the channel impulse response has a multipath delay spread, and its value is greater than the inverse of the transmitted signal waveform bandwidth. At this time, the received signal includes the multipath wave of the transmitted signal waveform that has undergone attenuation and time delay, so that the received signal is distorted. Frequency selective fading is caused by the time dispersion of the transmitted signal in the channel. This channel causes inter-symbol interference (ISI). Some frequency components of the received signal in the frequency domain have gained greater gain than others.

As shown in Fig.3, for frequency selective fading, the bandwidth of the transmitted signal spectrum $S(f)$ is greater than the coherent bandwidth B_c of the channel. It can be seen from the frequency domain that when different frequencies obtain different gains, the channel will have frequency selection. When the multipath delay approaches or exceeds the period of the transmitted signal, frequency selective fading will occur. Since the bandwidth of the signal $s(t)$ is greater than the channel impulse response bandwidth, the frequency selective fading channel is also called a wideband channel. As time changes, the channel gain and phase of the signal $s(t)$ within the frequency spectrum also change, resulting in time-varying distortion of the received signal $r(t)$.

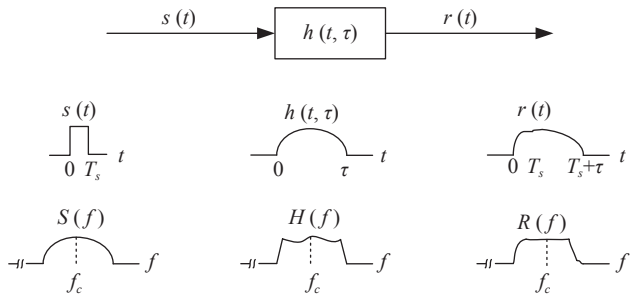

Fig. 3. Characteristics of frequency selective fading channels.

Due to the subcarriers of OFDM system are orthogonal to each other, they are independent of each other when transmitting in the channel, and the attenuation in the channel is different. Combining observation of multiple subcarriers can improve the stability and accuracy of ranging and positioning. Under normal communication conditions, the sub-signal bandwidth of orthogonal frequency division multiplexing system is smaller than the relevant bandwidth of the channel, therefore, the fading of each sub-channel can be regarded as consistent with flat fading, so it has good multipath resistance.

III. Proposed Ranging System

In OFDM communication system, multiple sub-carriers can be provided for communication ranging. Taking triple carriers as an example, the OFDM ranging method proposed in this paper is as follows. It uses triple subcarriers f_0, f_1, f_2 which are specifically used for ranging, and the remaining subcarriers are used to transmit data just like the communication system. As shown in Fig.4, suppose there are N subcarriers in an OFDM system, and f_0 is the subcarrier with the smallest baseband frequency. The subcarrier frequency is determined in advance during positioning, and the three subcarrier data are skipped during parallel-to-serial conversion at the receiver for ranging alone.

When an OFDM signal passes through a wireless multi-path channel, frequency selective fading causes several groups of subcarriers in the OFDM symbol to have larger fading. The large fading in the frequency response of this channel will distort the information carried on adjacent subcarriers. Therefore, maximizing the frequency difference when selecting subcarriers for positioning can resist frequency selective fading. In frequency selective fading, the coherence bandwidth of the channel is smaller than the bandwidth of the signal. Therefore, different frequency components of the signal experience uncorrelated fading. At this time, the use of multiple subcarriers can improve the stability of observation. When one subcarrier signal produces large fading, other subcarriers are less affected. Combined observation can ensure the accuracy of observation results.

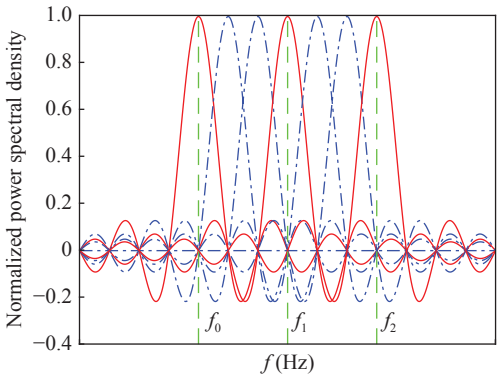

Fig. 4. OFDM power spectrum diagram.

Fig.5 shows the structure of the ranging frame. The "Head" field is one byte long. The "Check sum" field is one byte long and is used for data validation. The "Position information" field consists of the longitude, latitude, and altitude of the base station, each occupying eight bytes, totaling 24 bytes. The "Device ID" is one byte, which indicates the signal transmitted by which base station. The "Subcarrier ID" is one byte and is used to indicate which subcarrier signal. The ranging signal delay is used to measure the distance between the receiver and the base station. The three subcarriers used for ranging can not only improve the ranging accuracy but also ensure the accuracy of the coordinate data of the ranging base station. Occupying three subcarriers at the same time will not cause much impact on the communication capacity of the original communication system.

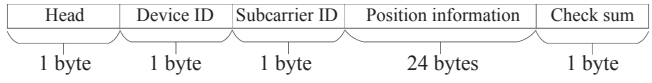

Fig. 5. Ranging data frame.

1. OFDM ranging scheme

The system model in the OFDM ranging scheme is shown in Fig.6, which refers to the OFDM communication system model. The ranging system is mainly divided into two parts: the transmitting terminal and the receiving terminal.

The input high-speed data stream is decomposed into a plurality of low-speed data streams. Each sub-data stream is modulated by orthogonal sub-carriers, and the combined data stream is transmitted through the channel. After receiving the signal, the receiver demodulates the combined data stream with each group of orthogonal carriers. After parallel-serial conversion, the original high-speed data stream is recovered. The down-converted signal and the demodulated signal are used for position estimation.

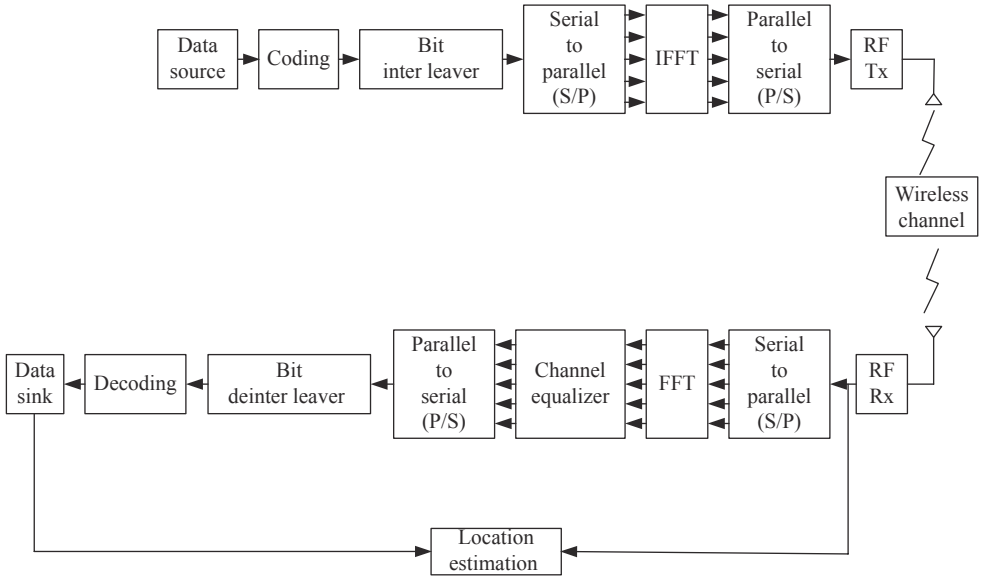

Fig. 6. OFDM ranging scheme.

2. Signal and channel model

The transmission ranging signal of the OFDM system is expressed as

$$s_0(t) = s(t)g_0(t) = \sum_{k=0}^{N-1} A_k \cos\left(2\pi\left(f_c + f_k\right)t + \phi_k\right) g_0(t) \quad (1)$$

where N is the number of subcarriers, f_c is the central frequency, f_k is the baseband frequency of the th subcarrier and can be expressed as $f_k = (2k - N{+}1)\Delta f/2$, A_k and ϕ_k are the amplitude and phase of the kth subcarrier. The unit rectangular pulse $g_0(t)$ is non-zero for $t \in [-T_{\mathrm{CP}}, T]$ where $T = 1/\Delta f$ and T_{CP} is the length of the cyclic prefix. Δf is the subcarrier spacing of ranging signal.

Due to the reflection of signals from indoor walls, there are multipath signals in the environment, so the signal received by the receiver can be written as

$$x(t) \triangleq [h(t) * s_0(t)]\, g(t) \quad (2)$$

$h(t)$ is the impulse response of the multipath channel and can be written as

$$h(t) = \sum_{l=0}^{L-1} a_l \delta\left(t - \tau_l\right) \quad (3)$$

where $n(t)$ is the additive white Gaussian noise with two-sided spectrum density of $N_0/2$, L is the number of arrival paths, a_l and τ_l are the amplitude and propagation delay of the pth path, L is the number of arrival paths, τ_0 is the propagation delay of the first path and can be expressed as $\tau_0 = R/c$, where R is the distance between the transmitter and the base station, c is the speed of light. Therefore, the estimation of the distance can be converted into the estimation of the delay. The unknown parameters to be estimated can be organized as $\theta = \left[\tau^{\mathrm{T}}, \alpha^{\mathrm{T}}\right]^{\mathrm{T}}$, where $\tau = [\tau_0, \tau_1, \ldots, \tau_{L-1}]^{\mathrm{T}}$ and $\alpha = [\alpha_0, \alpha_1, \ldots, \alpha_{L-1}]^{\mathrm{T}}$. The received signal without the cyclic prefix is expressed as

$$r(t) = x(t) + n(t)g(t) \quad (4)$$

where $g(t)$ is a unit rectangular pulse which is non-zero in $[0, T]$. The Fourier transform of $r(t)$ can be expressed as $R(f) = X(f) + N(f)$. Where $X(f)$ is the Fourier transform of $x(t)$ which can be written as

$$X(f) = \sum_{k=0}^{N-1} \frac{A_k}{2} \left[H\left(f_c + f_k\right) G\left(f - f_c - f_k\right) \mathrm{e}^{\mathrm{j}\phi_k} + H\left(-f_c - f_k\right) G\left(f + f_c + f_k\right) \mathrm{e}^{-\mathrm{j}\phi_k}\right] \quad (5)$$

The Fourier transform of $r(t)$ is expressed as

$$R(f) = R\left(f\right) = X\left(f\right) + N\left(f\right) = \frac{TA_k}{2} \sum_{l=1}^{L} \alpha_l \mathrm{e}^{-\mathrm{j}(2\pi f \tau_l - \phi_k)} + N(f) \quad (6)$$

where $G(f)$, $H(f)$, and $N(f)$ are the Fourier transforms.

3. Ranging positioning analysis

When using our proposed positioning method, i.e. four base stations to locate a target point, the following four situations generally occur.

- Case 1: Each observation is within the normal error range, which is in line with the statistical characteristics of the measurement error.

In this case, the four ranging circles may not con-

verge at one point, but form a converging area with a relatively small area. The ideal situation is that the four circles meet at one point. This situation only occurs when all positioning base station systems have no errors.

• Case 2: One of the base stations has a large ranging error, and the other base stations have normal ranging errors.

This situation usually occurs in an environment where a certain signal propagation path is blocked. If in this case the solution of the anchor point equations directly will lead to an increase in the uncertainty of the results. In order to get better positioning results, the best way is to find the abnormal ranging device first and then remove it from the solving equations; the next best method is to weight the processing to reduce the impact on the positioning results.

• Case 3: All ranging circles do not form an intersection area.

This situation of no intersection area is caused by the signals of the four ranging devices being blocked. It does not have a least squares solution. At this time, the least squares cannot converge, and the correct positioning point cannot be found.

• Case 4: Only two base stations have ranging information.

This situation occurs when two base stations are able to perform normal ranging normally, and the other two base stations are unable to operate normally and cannot perform normal ranging. In this case, there are only two ranging information. In three-dimensional space, only two ranging information cannot be solved. If approximate positioning points are required, additional constraint information needs to be added.

IV. Triple-Frequency Combining Observation Models

As there is a certain correlation between the errors of the observation values with different frequencies, the combination observation values formed by linear combination of multiple observation values can achieve the purpose of weakening various errors and improving positioning accuracy. Based on OFDM signals and multipath channels, a triple-frequency observation model is proposed to improve the accuracy of receiver observation.

In the process of positioning and ranging, the delay time of the signal actually corresponds to the change of the signal carrier phase. As shown in Fig.7, the phase of the ranging signal when it is emitted from the transmitting end is ϕ_S, and the phase when it is received by the receiver is ϕ_E. The phase difference of the signals can be expressed as

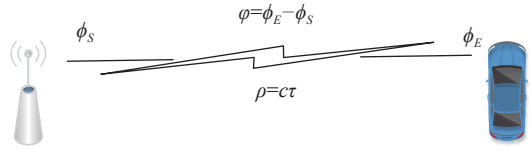

Fig. 7. Carrier ranging process.

$$\varphi = \phi_E - \phi_S \tag{7}$$

The distance between receiver and transmitter is expressed as

$$\rho = c\tau = \varphi\lambda \tag{8}$$

where ρ is the distance, c is the speed of light, τ is the signal delay, and λ is the carrier wavelength. For a 5 GHz carrier wave, one wavelength is 0.06 m, so the ambiguity of the receiver observation will lead to ranging errors of more than one wavelength. Therefore, multi-subcarrier observation model is used to improve the accuracy of receiver observation.

The frequencies of the ranging subcarriers are determined in advance to be f_0, f_1, and f_2. Reach the receiver after propagating through the wireless channel. The observation of the ranging subcarrier phase measured by the receiver can be expressed as

$$\varphi_i = \frac{1}{\lambda_i}\rho - N_i + \varepsilon_i \tag{9}$$

In equation (9), $i = 1, 2, 3$ represents different carrier frequencies, φ_i represents the carrier phase observation value, ρ represents the true value of the geometric distance from the base station transmitter to the receiver, and $\mathcal{E}_i$ is the carrier phase noise of the corresponding frequency. N_i is the integer periodic ambiguity of the observed value. The observation values of the OFDM subcarrier phases of different frequencies represented by (10) are linearly combined, and the observation values of the combined subcarrier phases are expressed as

$$\begin{aligned}\varphi_{ijk} &= i\varphi_1 + j\varphi_2 + k\varphi_3 \\ &= \left(\frac{i}{\lambda_1} + \frac{j}{\lambda_2} + \frac{k}{\lambda_3}\right)\rho \\ &\quad - (iN_1 + jN_2 + kN_3) \\ &\quad + (i\varepsilon_1 + j\varepsilon_2 + k\varepsilon_3)\end{aligned} \tag{10}$$

In (10), φ_{ijk} is the carrier phase combined observation value, and (i, j, k) is the combined observation value coefficient. In order to ensure the whole cycle characteristic of the combined ambiguity of the combined observation value, which can be writtened as $N_{ijk} = iN_1 + jN_2 + kN_3$. i, j, k are non-zero integers, and

$$\frac{1}{\lambda_{ijk}} = \frac{i}{\lambda_1} + \frac{j}{\lambda_2} + \frac{k}{\lambda_3} \tag{11}$$

The wavelength of the combined phase combination observations is solved as

$$\lambda_{ijk} = \frac{\lambda_1\lambda_2\lambda_3}{i\lambda_2\lambda_3 + j\lambda_1\lambda_3 + k\lambda_1\lambda_2} \tag{12}$$

Then equation (10) can be simplified as

$$\varphi_{ijk} = \frac{1}{\lambda_{ijk}}\rho - N_{ijk} + \varepsilon_{ijk} \tag{13}$$

where N_{ijk} is the ambiguity of the combined observations and $\varepsilon_{ijk} = i\varepsilon_1 + j\varepsilon_2 + k\varepsilon_3$ is the noise of the combined observations.

Due to the linear combination, the noise amplification factor of the combined observation value will be greater than the noise amplification factor corresponding to the original carrier observation value. The formula of the noise amplification factor in units of length is rewritten into the frequency form:

$$\bar{n}_{ijk} = \frac{\sqrt{i^2 + j^2 + k^2}}{if_1 + jf_2 + kf_3} \to \min \tag{14}$$

In the coefficient space (i, j, k), the combination that satisfies the above formula forms a straight line.

$$\begin{bmatrix} i \\ j \\ k \end{bmatrix} = t \begin{bmatrix} f_i \\ f_j \\ f_k \end{bmatrix} \tag{15}$$

It can be known from (15) that the noise amplification factor in terms of length is the smallest when the combination coefficient is proportional to the subcarrier frequency.

Based on (13), we can obtain the distance from the phase of the signal:

$$\rho = (N_{ijk} + \varphi_{ijk} + \varepsilon_{ijk})\,\lambda_{ijk} = c\tau_0 \tag{16}$$

Therefore, in the OFDM ranging system, the combination coefficient is determined according to the predetermined subcarrier frequency to ensure that the result is affected by noise minimal. It is helpful to improve the accuracy of the ambiguity solution. The geometric distance between the transmitting end and the receiving end is calculated by combining the phase observations.

V. Proposed Positioning Algorithm

Positioning accuracy is closely related to the accuracy of ranging information [23]. Algorithms that use ranging information to calculate the receiver's three-dimensional coordinates usually require signals from four transmitters to locate. The receiver measures the distance from the four base stations and knows the coordinates of the base stations. The coordinates of the receiver are obtained through geometric positioning algorithm. Fig.8 illustrates the indoor positioning method. The receiver measures the distances R_1, R_2, R_3, R_4 and the coordinates of the base stations from the four base stations, and obtains the coordinates of the receiver through a geometric positioning algorithm. Geometric positioning methods, such as the least squares method, are closely related to positioning accuracy.

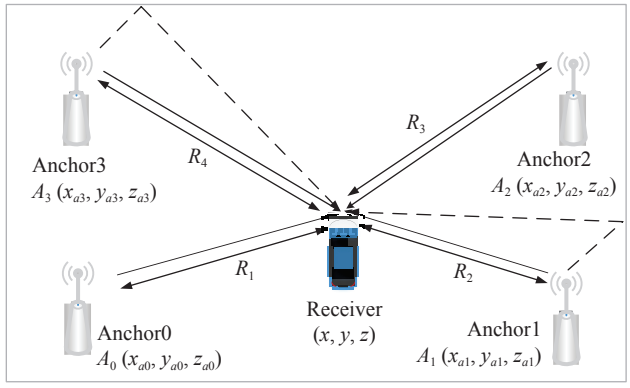

Fig. 8. Ranging data frame.

Since OFDM usually uses antenna arrays, multiple antennas can be used for positioning in one transmitter, which can reduce the number of transmitters required for positioning compared with common methods. The positioning algorithm for multiple antennas and multiple base stations is the same, except that the position coordinates of the antennas are substituted for the position coordinates of the base stations. Next section proves the positioning accuracy of this system.

1. Positioning algorithm

The algorithm can be summarized as follows.

1) Determine the subcarrier frequency used for ranging.

2) The receiver broadcasts the request positioning signal and prepares to receive it.

3) The receiver multiple receives positioning signals from transmitters.

4) Extracting subcarrier signals and combine subcarrier observations.

5) Get the distances between the receiver and the transmitters.

6) Calculate receiver coordinates using geometric algorithms mathematical model of base station positioning.

As shown in the Fig.8, the four anchors are deployed in advance as base stations, and the position coordinates of the four anchors are calibrated and recorded as $A_0\,(x_{a0}, y_{a0}, z_{a0})$, $A_1\,(x_{a1}, y_{a1}, z_{a1})$, $A_2\,(x_{a2}, y_{a2}, z_{a2})$, and $A_3\,(x_{a3}, y_{a3}, z_{a3})$, respectively. At a certain

time k, the distances between the receiver and the four antennas are R_1, R_2, R_3, R_4, respectively.

The base station positioning principle is to measure the distance between a receiver and 3 or more base stations, and solve the distance equation to get the position coordinates of the measured receiver, which can be expressed as follows:

$$R(x,y,z)=\sqrt{(x-x_a)^2+(y-y_a)^2+(z-z_a)^2} \quad (17)$$

Among them, (x,y,z) is the receiver coordinate to be solved, (x_a,y_a,z_a) is the base station coordinate calibrated in advance, and R is the geometric distance between the receiver and base stations.

2. Nonlinear least squares iteration

According to the ranging information of the four base stations, the corresponding ranging equations can be obtained, and the coordinates of the target positioning can be obtained by solving the ranging equations. In this article, we use nonlinear least squares iteration to solve this ranging equations.

Assuming that the estimated value of the receiver coordinate is $\hat{\boldsymbol{\beta}}=(\hat{x},\hat{y},\hat{z})$, the first-order Taylor expansion of the ranging (17) at $\hat{\boldsymbol{\beta}}$ is obtained as

$$\begin{aligned}R(x,y,z)=R(\hat{x},\hat{y},\hat{z})+\frac{\partial R}{\partial x}\cdot(x-\hat{x})+\frac{\partial R}{\partial y}\cdot(y-\hat{y})\\+\frac{\partial R}{\partial z}\cdot(z-\hat{z})+\mathcal{O}\left(\hat{\boldsymbol{\beta}}\right)^2\end{aligned} \quad (18)$$

In order to facilitate expression and perform matrix operations, the following equation holds:

$$\Delta R=R(x,y,z)-R(\hat{x},\hat{y},\hat{z})=R-\hat{R} \quad (19)$$

$$\Delta x=x-\hat{x},\Delta y=y-\hat{y},\Delta z=z-\hat{z} \quad (20)$$

$$\hat{r}=\sqrt{(\hat{x}-x_a)^2+(\hat{y}-y_a)^2+(\hat{z}-z_a)^2} \quad (21)$$

According to (17)–(21) and the partial differential formula, the following equations can be obtained:

$$\frac{\partial R}{\partial x}=\frac{x-\hat{x}}{\hat{r}},\frac{\partial R}{\partial y}=\frac{y-\hat{y}}{\hat{r}},\frac{\partial R}{\partial z}=\frac{z-\hat{z}}{\hat{r}} \quad (22)$$

To simplify matrix calculations, equation (22) can be represented using vector $\boldsymbol{u}$ as follows:

$$\boldsymbol{u}=\left[\frac{\partial R}{\partial x},\frac{\partial R}{\partial y},\frac{\partial R}{\partial z}\right] \quad (23)$$

If there are m sets of ranging information, and the second order and above errors of (19) are discarded, the nonlinear ranging equation can be linearized into the following equations:

$$\begin{bmatrix}\Delta R_1\\ \Delta R_2\\ \vdots\\ \Delta R_m\end{bmatrix}=\begin{bmatrix}\frac{\partial R_1}{\partial x}&\frac{\partial R_1}{\partial y}&\frac{\partial R_1}{\partial z}\\ \frac{\partial R_2}{\partial x}&\frac{\partial R_2}{\partial y}&\frac{\partial R_2}{\partial z}\\ \vdots&\vdots&\vdots\\ \frac{\partial R_m}{\partial x}&\frac{\partial R_m}{\partial y}&\frac{\partial R_m}{\partial z}\end{bmatrix}\cdot\begin{bmatrix}\Delta x\\ \Delta y\\ \Delta z\end{bmatrix} \quad (24)$$

Write (24) as a matrix, as follows:

$$\Delta\boldsymbol{R}=H\cdot\Delta\hat{\boldsymbol{\beta}} \quad (25)$$

where, $\Delta R=\begin{bmatrix}\Delta R_1\\ \Delta R_2\\ \vdots\\ \Delta R_m\end{bmatrix}$, $H=\begin{bmatrix}\frac{\partial R_1}{\partial x}&\frac{\partial R_1}{\partial y}&\frac{\partial R_1}{\partial z}\\ \frac{\partial R_2}{\partial x}&\frac{\partial R_2}{\partial y}&\frac{\partial R_2}{\partial z}\\ \vdots&\vdots&\vdots\\ \frac{\partial R_m}{\partial x}&\frac{\partial R_m}{\partial y}&\frac{\partial R_m}{\partial z}\end{bmatrix}$

$$\Delta\hat{\boldsymbol{\beta}}=\begin{bmatrix}\Delta x\\ \Delta y\\ \Delta z\end{bmatrix} \quad (26)$$

Finally, the least square solution of (25) is obtained as follows:

$$\Delta\hat{\beta}=\left(H^{\mathrm{T}}\cdot H\right)^{-1}\cdot H^{\mathrm{T}}\cdot\Delta R \quad (27)$$

H is the observation matrix, which is a Jacobian matrix. From (18)–(27), the solution process of the nonlinear least squares is given.

The specific solution steps are given below:

Step 1. Sets the initial value of the nonlinear least squares iteration. Set to $\hat{\boldsymbol{\beta}}=[0,0,0]^{\mathrm{T}}$ or the estimated value at the previous moment, i.e., $\hat{\beta}=\hat{\beta}_{k-1}$.

Step 2. Calculate the prior ranging error ΔR by using (19).

Step 3. Calculate the cosine vector u and the observation matrix H of the ranging direction by using (21) and (22).

Step 4. Use (26) to solve the state estimation error vector $\Delta\hat{\beta}$.

Step 5. According to (27), update the current iteration state: $\hat{\beta}=\hat{\beta}+\Delta\hat{\beta}$.

Step 6. Judge whether convergence. The convergence condition is: $\left\|\Delta\hat{\beta}\right\|_2\le\mathrm{Th}$, generally $\mathrm{Th}=10^{-6}$.

If the convergence condition is satisfied, then $\hat{\beta}$ at this time is the state least squares estimation value of the current epoch, and step 7 is continued. Otherwise, return to step 2 and continue the iteration. A number of iterations can be set to prevent a dead loop from always failing to meet the convergence conditions. Generally, convergence can be achieved in 3–5 iterations.

Step 7. Calculate the estimation error.

VI. Analysis of Positioning Accuracy

CRLB can be used to calculate the best estimation accuracy that can be obtained in unbiased estimation, so it is often used to calculate the best estimation accuracy that can be achieved by theory. The simplest form of CRLB is the reciprocal of Fisher information. This section analyzes the ranging accuracy by calculating CRLB. Based on the signal and channel models in Section III, the likelihood function of θ satisfies the following conditions

$$\Lambda(R(f);\boldsymbol{\theta}) \propto \exp\left(-\frac{1}{N_{\mathrm{f}}}\left\|R(f)-\frac{TA_k}{2}\sum_{l=1}^{L}\alpha_l \mathrm{e}^{-\mathrm{j}(2\pi f\tau_l-\phi_k)}\right\|^2\right) \tag{28}$$

where $\theta=\left[\tau^{\mathrm{T}},\alpha^{\mathrm{T}}\right]^{\mathrm{T}}$, $\boldsymbol{\theta}$ is a matrix of signal delay and signal amplitude. Since the noise components at different samples in $\mathcal{R}_{\mathrm{f}}$ are i.i.d. complex Gaussian, $\Lambda(\cdot;\boldsymbol{\theta})$ can be expressed as the product of the likelihood functions at different sampled frequencies. According to the log-likelihood function, the score function is calculated. Calculate the second-order moment of the score function. Fisher information can be obtained by

$$F_\theta=\begin{bmatrix} F_{\tau\tau} & F_{\tau a} \\ F_{a\tau} & F_{aa}\end{bmatrix} \tag{29}$$

where

$$F_\theta=\mathbb{E}_{\mathcal{R}_{\mathrm{f}}}\left\{-\frac{\partial^2\ln\Lambda\left(\mathcal{R}_{\mathrm{f}};\boldsymbol{\theta}\right)}{\partial\boldsymbol{\theta}\partial\boldsymbol{\theta}^{\mathrm{T}}}\right\} \tag{30}$$

It can be known from the above formula that the Fisher information of the positioning parameter is independent of the symbol phase. The mean squared error (MSE) of θ is bounded as

$$\mathbb{E}_{\mathcal{R}_{\mathrm{f}}}\left\{(\hat{\boldsymbol{\theta}}-\boldsymbol{\theta})(\hat{\boldsymbol{\theta}}-\boldsymbol{\theta})^{\mathrm{T}}\right\}\succeq F_{\boldsymbol{\theta}}^{-1} \tag{31}$$

$F_{\boldsymbol{\theta}}$ can be expressed as the sum of the FIMs for all subcarriers as follows:

$$F_\theta=\sum_{k=0}^{N-1}\left(F\left(f_{\mathrm{c}}+f_k\right)+F\left(-f_{\mathrm{c}}-f_k\right)\right) \tag{32}$$

The FIM at frequency $F(f)$ can be calculated from (28), (30) shown as

$$F(f)=\mathbb{E}_{\mathcal{R}_{\mathrm{f}}}\left\{-\frac{\partial^2\ln\Lambda(R(f);\boldsymbol{\theta})}{\partial\boldsymbol{\theta}\partial\boldsymbol{\theta}^{\mathrm{T}}}\right\} \tag{33}$$

After some algebra, elements in $F(f)$ can be expressed as follows:

$$\mathbb{E}_{\mathcal{R}_{\mathrm{f}}}\left\{-\frac{\partial^2\ln\Lambda(R(f);\boldsymbol{\theta})}{\partial\tau_i\partial\tau_j}\right\}=\frac{\alpha_i\alpha_j T}{N_0}P_k(2\pi f)^2\cos\left(2\pi f\tau_{ij}\right) \tag{34}$$

$$\mathbb{E}_{\mathcal{R}_{\mathrm{f}}}\left\{-\frac{\partial^2\ln\Lambda(R(f);\boldsymbol{\theta})}{\partial\tau_i\partial\alpha_j}\right\}=-\frac{\alpha_i T}{N_0}P_k(2\pi f)\sin\left(2\pi f\tau_{ij}\right) \tag{35}$$

$$\mathbb{E}_{\mathcal{R}_{\mathrm{f}}}\left\{-\frac{\partial^2\ln\Lambda(R(f);\boldsymbol{\theta})}{\partial\alpha_i\partial\alpha_j}\right\}=\frac{T}{N_0}P_k\cos\left(2\pi f\tau_{ij}\right) \tag{36}$$

where $\tau_{ij}=\tau_i-\tau_j$, $0\le i,j\le L-1$ and $P_k=A_k^2$ is the power of the kth subcarrier. As can be seen from (34), (35), and (36), FIM is independent of the phase of the data. The CRLB for the mean-square estimation error of τ_0 is $\sigma_{\mathrm{CRB}}^2(\tau_0)$. Substitute the above formula into (33), the CRLB can be written as

$$\mathbb{E}_{\mathcal{R}_f}\left[\left(\hat{\tau}_0-\tau_0\right)^2\right]\ge\sigma_{\mathrm{CRB}}^2(\tau_0)=\left[F_\theta^{-1}\right]_{1,1} \tag{37}$$

where $[F_\theta]_{1,1}$ is the equivalent Fisher information (EFI) of τ_0. Since f_{c} is much larger than the bandwidth for most OFDM signals, we approximate the elements in $F_{\boldsymbol{\theta}}$ except for $[F_\theta]_{1,1}$ as follows:

$$\sum P_k\omega_{\mathrm{ck}}^2\cos\left(\omega_{\mathrm{ck}}\tau_{ij}\right)\approx\omega_{\mathrm{c}}^2\sum P_k\cos\left(\omega_{\mathrm{ck}}\tau_{ij}\right) \tag{38}$$

$$\sum P_k\omega_{\mathrm{ck}}\sin\left(\omega_{\mathrm{ck}}\tau_{ij}\right)\approx\omega_{\mathrm{c}}\sum P_k\sin\left(\omega_{\mathrm{ck}}\tau_{ij}\right) \tag{39}$$

$$\sum P_k\omega_{\mathrm{ck}}^2\approx 2\omega_{\mathrm{c}}^2E_{\mathrm{T}}/T \tag{40}$$

Due to multipath effect, the first path in the received signal is affected by the subsequent path, which leads to the decrease of ranging performance [23]. Since the second path has the greatest influence on the main path signal, this paper mainly analyzes the two-path channel in the following. In the two-path channel, the approximate value of EFI for ranging based on (38), (39), and (40) is given by

$$[F_\theta]_{1,1}=\frac{2\alpha_0^2T}{N_0}\left(\sum_{k=0}^{N-1}P_k\omega_{\mathrm{ck}}^2-\frac{\omega_{\mathrm{c}}^2T}{2E_{\mathrm{T}}}h\right) \tag{41}$$

where

$$h=\left(\sum_{k=0}^{N-1}P_k\cos\left(\omega_k\tau\right)\right)^2+\left(\sum_{k=0}^{N-1}P_k\sin\left(\omega_k\tau\right)\right)^2 \tag{42}$$

and $\tau=\tau_1-\tau_0$. The first term of the polynomial in (41) is the EFI of ranging in the single path channel. The second term in (41) represents the effect of path overlap of multipath channels. We will quantify the impact of OFDM channel parameters on EFI based on (42). Assuming that there is a total energy constraint, the energy of the FFT part of one OFDM symbol can be

constrained as

$$\int_0^T s^2(t)\mathrm{d}t = \frac{T}{2}\sum_{k=0}^{N-1} P_k \le E_T \tag{43}$$

where E_T is the maximum transmit energy. Based on (41) and (42), EFI can be rewritten as

$$[F_\theta]_{1,1} = \frac{2\alpha_0^2 T}{N_0}\left[\left(\frac{2E_{\mathrm{T}}}{T} - \frac{Th}{2E_{\mathrm{T}}}\right)\omega_{\mathrm{c}}^2 + \sum_{k=0}^{N-1} P_k\left(2\omega_{\mathrm{c}}\omega_k + \omega_k^2\right)\right] \tag{44}$$

Therefore, $[F_\theta]_{1,1} \propto f_c$. EFI can be rewritten as a function related to M and Δf.

$$[F_\theta]_{1,1} = \frac{2\alpha_1^2}{N_0}\left[2E_{\mathrm{T}}\omega_{\mathrm{c}}^2 + \frac{E_{\mathrm{T}}\Delta\omega^2}{6}\left(4M^2-1\right) - \frac{E_{\mathrm{T}}\omega_{\mathrm{c}}^2}{2M^2}\frac{\sin^2(M\Delta\omega\tau)}{\sin^2(\Delta\omega\tau/2)}\right] \tag{45}$$

where $\omega_c = 2\pi f_c$, $\omega_k = 2\pi f_k$, and $\Delta\omega = 2\pi\Delta f$. Thus, the EFI for ranging can be increased by using larger subcarrier spacing. According to the definition of CRLB, as shown in (45), this shows that the larger the subcarrier spacing is, the smaller the CRLB will be.

VII. Simulation Results

In this section, we analyze the influence of signal and channel parameters on OFDM ranging and position accuracy. We consider an OFDM system with 121 subcarriers. The central frequency is 5 GHz and the subcarrier spacing is 240 kHz. One of the parameters can be changed in the experiment. Four base stations are set on the same horizontal plane at a height of 2 m with coordinates of (0,0,2) (0,20,2) (20,0,2) (20,20,2). 100 Monte Carlo experiments were carried out in 100 randomly selected locations on the base station plane to calculate MSE and RMSE.

As shown in Fig.9, the larger the frequency spacing used for positioning, the smaller the CRLB, and the higher the ranging accuracy. It shows that the proposed method has better performance in multipath environment. Therefore, the frequency difference of the three subcarriers should be chosen as large as possible. Select the 1st, 61st and 121st of 121 subcarriers. At this time, the subcarrier spacing is 14.4 MHz, and the corresponding MSE is 0.0029. The results of using the positioning algorithm are slightly worse than CRLB, but remain basically the same.

As shown in Fig.10, the larger the f_c, the Smaller the CRLB of the ranging information, and the Fisher information is proportional to the square of the f_c. The

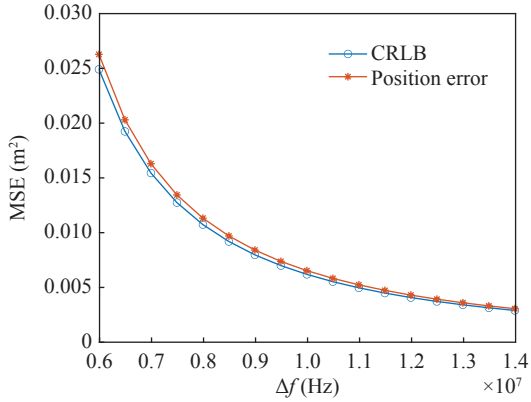

Fig. 9. CRLB baseline and MSE under different Δf.

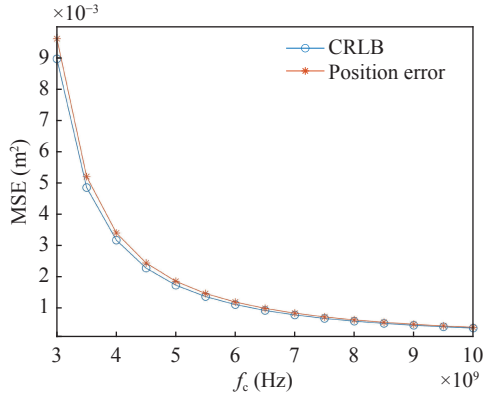

Fig. 10. CRLB baseline and MSE under different f_c.

MSE is 0.0096 at 3 GHz and 0.0012 at 6 GHz. The f_c becomes larger, the ranging accuracy will perform better. Therefore, the proposed method has better performance in high frequency signals.

As shown in Fig.11, the larger N is, the smaller the CRLB is, that is, the more accurate the ranging information is. In accordance with the previous section, Fisher information is proportional to the square of N. However, a larger N means that the positioning signal needs to occupy more subcarriers. At this time, the number of subcarriers occupied by the communication data becomes smaller, that is, the communication capacity is reduced. Therefore, when three subcarriers are selected for positioning, MSE is increased by 80%, and at the same time, it does not occupy too much communication resources, thus ensuring that the original communication capacity is not affected too much.

As shown in Fig.12, the RMSEs of ML algorithms of various indoor positioning technologies are compared. These technologies are based on ranging positioning methods. When using the same ML positioning algorithm, ranging accuracy is positively related to positioning. Under the condition of a high signal-to-noise ratio, the positioning accuracy ratio of RFID decreases rapidly. The multi-frequency positioning accuracy pro-

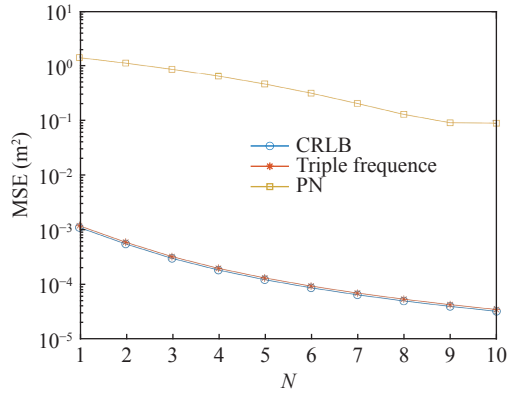

Fig. 11. MSE of different methods when the number of subcarriers changes.

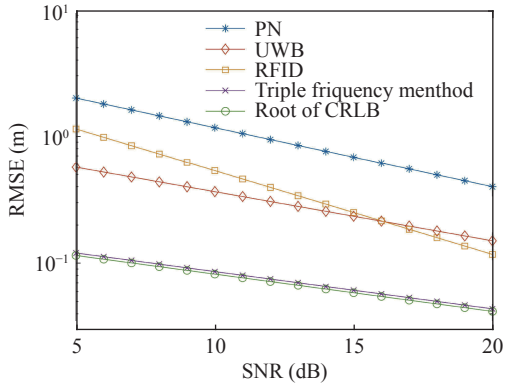

Fig. 12. RMSE of different positioning methods.

posed in this paper is much better than indoor positioning methods such as PN, UWB and RFID.

Fig.13 shows the horizontal dilution of precision (HDOP). Four base stations are set on the same horizontal plane at a height of 2 m with coordinates of (0,0,2) (0,20,2) (20,0,2) (20,20,2). Where coordinates are in meters. The positioning effect in the middle position is worse than that in the peripheral position. Since the receiver has similar angles to the four base stations at the center point, HDOP is large and the calculation error is large. Therefore, although OFDM can use multiple antennas of one base station to locate, its accuracy is not as good as that of four base stations.

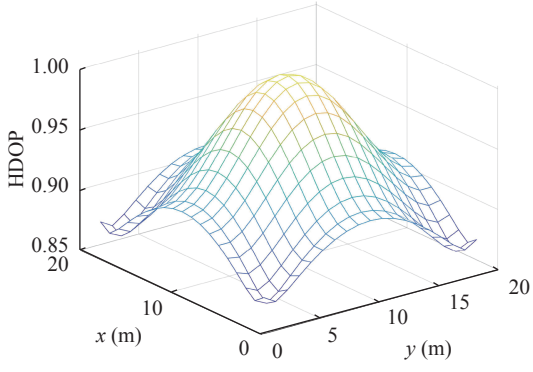

Fig. 13. HDOP of OFDM position system.

VIII. Conclusions

This paper introduces a method for multi-frequency ranging using sub-carriers in an OFDM communication system. The integrated OFDM communication and positioning system is first introduced, including ranging subcarrier selection and ranging frame format. Because the ranging positioning only needs to know the position coordinates of the base station, the base station coordinates of the transmitted signal are included in the ranging frame. Subsequently, a ranging signal model transmitted by the base station was established, and the CRLB of the ranging was proved. Finally, simulation experiments prove that the RMSE of the ranging and positioning system has superior accuracy compared with other positioning methods. Under experimental conditions, RMSE can reach about 5 cm.

References

[1] D. L. Wang and F. M. Ghannouchi, "Handset-based positioning system for injured fireman rescue in wildfire fighting," *IEEE Systems Journal*, vol.6, no.4, pp.603–615, 2012.

[2] H. L. Qin, P. Liu, L. Cong, *et al.*, "Triple-frequency combining observation models and performance in precise point positioning using real BDS data," *IEEE Access*, vol.7, pp.69826–69836, 2019.

[3] B. Rokaha, B. P. Gautam, and T. Kitani, "Building a reliable and cost-effective RTK-GNSS infrastructure for precise positioning of IoT applications," in *Proceedings of the 2019 Twelfth International Conference on Mobile Computing and Ubiquitous Network*, Kathmandu, Nepal, pp.1–4, 2019.

[4] N. Warakagoda, J. Dirdal, and E. Faxvaag, "Fusion of LiDAR and camera images in end-to-end deep learning for steering an off-road unmanned ground vehicle," in *Proceedings of the 2019 22th International Conference on Information Fusion*, Ottawa, ON, Canada, pp.1–8, 2019.

[5] J. W. Gong, Y. H. Jiang, G. M. Xiong, *et al.*, "The recognition and tracking of traffic lights based on color segmentation and camshift for intelligent vehicles," in *Proceedings of 2010 IEEE Intelligent Vehicles Symposium*, La Jolla, CA, USA, pp.431–435, 2010.

[6] X. M. Zhao, P. P. Sun, Z. G. Xu, *et al.*, "Fusion of 3D LIDAR and camera data for object detection in autonomous vehicle applications," *IEEE Sensors Journal*, vol.20, no.9, pp.4901–4913, 2020.

[7] L. C. Bento, R. Parafita, and U. Nunes, "Inter-vehicle sensor fusion for accurate vehicle localization supported by V2V and V2I communications," in *Proceedings of the 2012 15th International IEEE Conference on Intelligent Transportation Systems*, Anchorage, AK, USA, pp.907–914, 2012.

[8] R. C. Xu and T. Jiang, "Keeping track of position and cell residual dwell time of cellular networks using HSMM structure and cell-id information," in *Proceedings of 2012 IEEE International Conference on Communications*, Ottawa, ON, Canada, pp.6411–6415, 2012.

[9] F. Xiao, Z. Q. Wang, N. Ye, *et al.*, "One more tag enables fine-grained RFID localization and tracking," *IEEE/ACM Transactions on Networking*, vol.26, no.1, pp.161–174, 2018.

[10] N. Li, C. Shen, K. Zhang, *et al.*, "The TDOA algorithm based on BP neural network optimized by cuckoo search,"

in *Proceedings of 2019 International Conference on Robots & Intelligent System*, Haikou, China, pp.539–542, 2019.

[11] M. Ali, R. K. Rao, and V. Parsa, "PAPR reduction in OFDM system using new method for generating pseudo-random sequence for SLM technique," in *Proceedings of 2018 IEEE Canadian Conference on Electrical & Computer Engineering*, Quebec, QC, Canada, pp.1–4, 2018.

[12] L. Q. Gui, M. X. Yang, H. Yu, *et al.*, "A Cramer-Rao lower bound of CSI-based indoor localization," *IEEE Transactions on Vehicular Technology*, vol.67, no.3, pp.2814–2818, 2018.

[13] Q. W. Song, S. T. Guo, X. Liu, *et al.*, "CSI amplitude fingerprinting-based NB-IoT indoor localization," *IEEE Internet of Things Journal*, vol.5, no.3, pp.1494–1504, 2018.

[14] Z. Li, L. E. Luo, G. H. Sheng, *et al.*, "UHF partial discharge localisation method in substation based on dimension-reduced RSSI fingerprint," *IET Generation, Transmission & Distribution*, vol.12, no.2, pp.398–405, 2018.

[15] D. L. Wang and M. Fattouche, "OFDM transmission for time-based range estimation," *IEEE Signal Processing Letters*, vol.17, no.6, pp.571–574, 2010.

[16] T. H. Wang, Y. Shen, S. Mazuelas, *et al.*, "Bounds for OFDM ranging accuracy in multipath channels," in *Proceedings of 2011 IEEE International Conference on Ultra-Wideband*, Bologna, Italy, pp.450–454, 2011.

[17] D. L. Wang, F. M. Ghannouchi, Y. Ding, *et al.*, "70% energy saving in wireless positioning systems: non-data-bearing OFDM transmission replaces non-pulse-shaping PN transmission," *IEEE Systems Journal*, vol.9, no.3, pp.664–674, 2015.

[18] W. H. Dai, Y. Shen, and M. Z. Win, "Distributed power allocation for cooperative wireless network localization," *IEEE Journal on Selected Areas in Communications*, vol.33, no.1, pp.28–40, 2015.

[19] W. W. L. Li, Y. Shen, Y. J. Zhang, *et al.*, "Robust power allocation for energy-efficient location-aware networks," *IEEE/ACM Transactions on Networking*, vol.21, no.6, pp.1918–1930, 2013.

[20] T. van Nguyen, Y. Jeong, H. Shin, *et al.*, "Least square cooperative localization," *IEEE Transactions on Vehicular Technology*, vol.64, no.4, pp.1318–1330, 2015.

[21] A. G. Li and F. Z. Luan, "An improved localization algorithm based on CHAN with high positioning accuracy in NLOS-WGN environment," in *Proceedings of the 2018 10th International Conference on Intelligent Human-Machine Systems and Cybernetics*, Hangzhou, China, pp.332–335, 2018.

[22] D. L. Wang, M. Fattouche, F. M. Ghannouchi, *et al.*, "Quasi-optimal subcarrier selection dedicated for localization with multicarrier-based signals," *IEEE Systems Journal*, vol.13, no.2, pp.1157–1168, 2019.

[23] Y. Shen and M. Z. Win, "Fundamental limits of wideband localization—Part I: a general framework," *IEEE Transactions on Information Theory*, vol.56, no.10, pp.4956–4980, 2010.

LI Wengang received the B.E. degree in communication and information systems from Xidian University. He is currently an Associate Professor with the School of Communication Engineering, Xidian University. His research interests include navigation and positioning, broadband wireless communication, massive MIMO technology, networking technology and its application.

XU Yaqin received the B.E. degree in electronic engineering from Xidian University. She is currently pursuing the M.S. degree with the School of Communication Engineering, Xidian University. Her research interests include vehicle navigation and positioning.

ZHANG Chenmeng received the B.E. degree in electronic information science and technology from Jinan University. She is currently pursuing the M.S. Degree with the School of Communication Engineering, Xidian University. Her research interests include indoor navigation and positioning.

TIAN Yiheng received the B.E. degree from Nanchang University of Communication Engineering. He is currently pursuing the M.S. degree with the School of Communication Engineering, Xidian University. His research interests include wireless communication and internet of vehicles.

LIU Mohan received the B.E. degree in electronic and information engineering from Jiliang University. He is currently pursuing the M.S. degree with the School of Communication Engineering, Xidian University. His research interests include vehicle navigation and positioning.

HUANG Jun (corresponding author) received the B.E. degree in automation, M.D. degree in military communication, and Ph.D. degree in information security all from PLA Electronic Engineering Institute. He is currently an Associate Professor at National University of Defense Technology. His research interests include wireless network security. (Email:huangjun0111@nudt.edu.cn)